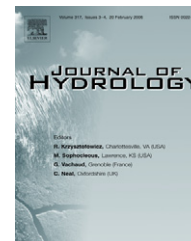




available at [www.sciencedirect.com](http://www.sciencedirect.com)



journal homepage: [www.elsevier.com/locate/jhydrol](http://www.elsevier.com/locate/jhydrol)



# Semi-analytical solution for flow in a leaky unconfined aquifer toward a partially penetrating pumping well

Bwalya Malama <sup>a,\*</sup>, Kristopher L. Kuhlman <sup>b</sup>, Warren Barrash <sup>a</sup>

<sup>a</sup> Center for Geophysical Investigation of the Shallow Subsurface, Department of Geosciences, Boise State University, 1910 University Drive, Boise, ID 83725, USA

<sup>b</sup> Department of Hydrology and Water Resources, University of Arizona, Tucson, AZ 85721, USA

Received 7 September 2007; received in revised form 10 March 2008; accepted 19 March 2008

## KEYWORDS

Unconfined aquifer;  
Confined aquifer;  
Aquitard;  
Leakage;  
Numerical inversion;  
Laplace–Hankel transform

**Summary** A semi-analytical solution is presented for the problem of flow in a system consisting of unconfined and confined aquifers, separated by an aquitard. The unconfined aquifer is pumped continuously at a constant rate from a well of infinitesimal radius that partially penetrates its saturated thickness. The solution is termed semi-analytical because the exact solution obtained in double Laplace–Hankel transform space is inverted numerically. The solution presented here is more general than similar solutions obtained for confined aquifer flow as we do not adopt the assumption of unidirectional flow in the confined aquifer (typically assumed to be horizontal) and the aquitard (typically assumed to be vertical). Model predicted results show significant departure from the solution that does not take into account the effect of leakage even for cases where aquitard hydraulic conductivities are two orders of magnitude smaller than those of the aquifers. The results show low sensitivity to changes in radial hydraulic conductivities for aquitards that are two or more orders of magnitude smaller than those of the aquifers, in conformity to findings of earlier workers that radial flow in aquitards may be neglected under such conditions. Hence, for cases where aquitard hydraulic conductivities are two or more orders of magnitude smaller than aquifer conductivities, the simpler models that restrict flow to the radial direction in aquifers and to the vertical direction in aquitards may be sufficient. However, the model developed here can be used to model flow in aquifer–aquitard systems where radial flow is significant in aquitards.

© 2008 Elsevier B.V. All rights reserved.

\* Corresponding author. Tel.: +1 208 426 2959; fax: +1 208 426 3888.  
E-mail address: [bmalama@cgiss.boisestate.edu](mailto:bmalama@cgiss.boisestate.edu) (B. Malama).

### Nomenclature

$K_{r,i}$	radial hydraulic conductivity of <i>i</i> th layer ( $\text{LT}^{-1}$ )	$r$	radial distance from pumping well (L)
$K_{z,i}$	vertical hydraulic conductivity of <i>i</i> th layer ( $\text{LT}^{-1}$ )	$d$	vertical distance from initial water table position to top of pumping well screen (L)
$S_{s,i}$	specific storage of <i>i</i> th layer ( $\text{L}^{-1}$ )	$l$	vertical distance from initial water table position to bottom of pumping well screen (L)
$S_Y$	unconfined aquifer specific yield,	$s_i$	drawdown in <i>i</i> th layer (L)
$\alpha_{r,i}$	radial hydraulic diffusivity of <i>i</i> th layer ( $\text{L}^2\text{T}^{-1}$ )	$Q$	pumping well discharge rate ( $\text{L}^3\text{T}^{-1}$ )
$\alpha_{z,i}$	vertical hydraulic diffusivity of <i>i</i> th layer ( $\text{L}^2\text{T}^{-1}$ )	$p$	Laplace transform parameter
$b_i$	vertical distance from initial water table position to bottom of <i>i</i> th layer (L)	$a$	Hankel transform parameter
$z$	vertical distance from initial water table position (L)	$t$	time since onset of pumping (T)

### Introduction

Leakage from adjacent aquitards has long been recognized to strongly impact the drawdown response of confined aquifers. The first major attempt to account for transient leakage in confined aquifer flow was made by Hantush and Jacob (1955), who presented the classical theory of leakage. To obtain their solution they assumed that the confined aquifer was bounded from below and above by aquitards of finite extent in which flow was entirely vertical and the effect of aquitard elastic storage was negligible. The assumption of negligible aquitard elastic storage leads to a steady-state aquitard flow problem that yields a linearly distributed hydraulic head in the aquitard. For confined aquifer flow, Hantush and Jacob (1955) adopted the assumption of horizontal flow. A major limitation of the classical theory of leakage is the assumption that aquitard storage has negligible effect on flow. Subsequently, Hantush (1960) presented the modified theory of leakage in which aquitard elastic storage was taken into account. As in classical leakage theory, flow in the aquitard was assumed to be vertical. Hantush (1960) presented numerical solutions only for early and late time. A more complete analytical solution for the problem confined aquifer flow with leakage was developed by Neuman and Witherspoon (1969a,b). They considered two confined aquifers, in which flow was assumed to be entirely horizontal, separated by an aquitard in which flow was assumed to be entirely vertical. To justify these assumptions, Neuman and Witherspoon (1969a) stated that “when the permeabilities of the aquifers are two or more orders of magnitude greater than that of the aquitard, errors introduced by this assumption are usually less than 5%”. Recently, Sepulveda (2008) developed a semi-analytical solution for flow in a leaky confined aquifer that allows for radial and vertical flow in the aquifer and aquitards. Their results from synthetic experiments indicate that more accurate estimates of hydraulic parameters are obtainable in this case than in the case where flow is assumed to be strictly radial in aquifers and strictly vertical in aquitards.

The effect of leakage on flow in an unconfined aquifer was first considered by Ehlig and Halepaska (1976) in their numerical (finite difference) solution of a coupled confined–unconfined aquifer problem. They adopted the Boulton (1954) model to simulate unconfined aquifer flow and the Hantush and Jacob (1955) model to simulate leakage through the common boundary of the system; no analytical

solution was developed. Others (Li, 2006) have analyzed data from multi-aquifer systems that include an unconfined aquifer using analytical solutions for confined aquifer flow with leakage. Zlotnik and Zhan (2005) developed an analytical solution for the problem of flow in a coupled unconfined aquifer–aquitard system, where the horizontal flow component in the aquitard is neglected. Zhan and Bian (2006) extended the work of Zlotnik and Zhan, 2005 and developed analytical and semi-analytical method for computing the leakage rate and volume induce by pumping based on the works of Hantush and Jacob (1955) and Butler and Tsou (2003). Zhan and Bian (2006) also neglect horizontal flow in the aquitard. The assumption of strictly vertical flow in the aquitard is based on the work of Neuman and Witherspoon (1969a) as discussed above. Additionally, Zlotnik and Zhan (2005) and Zhan and Bian (2006) restrict their solutions to the case of an aquitard of semi-infinite vertical extent. In this work, we develop a more general solution with respect to permissible values of aquitard hydraulic conductivity and aquitard thickness.

Malama et al. (2007) recently developed a semi-analytical solution for flow to a pumping well that fully penetrates the saturated thickness of a leaky unconfined aquifer underlain by an aquitard. The purpose of this work is to extend the semi-analytical solution of Malama et al. (2007) to a three-layered system consisting of an unconfined aquifer, an aquitard, and a confined aquifer, all of which are of infinite radial extent. The unconfined aquifer is pumped continuously at a constant rate from a well of infinitesimal radius that partially penetrates its saturated thickness. The solution is termed semi-analytical in the sense that exact analytical solution is obtained in the double Laplace–Hankel transform space, then inverted numerically. Water release due to water table decline is simulated in the manner of Neuman (1972). Flows in the three layers are coupled by imposing drawdown and vertical flux continuity conditions at the unconfined aquifer–aquitard and confined aquifer–aquitard boundaries. In this solution we do not neglect horizontal flow in the aquitard or vertical flow in the confined aquifer, as is usually assumed in leakage theories for confined aquifers (e.g. the multi-layer approach outlined in Bruggeman (1999, p. 637) or given by Lenoach et al. (2004) in the petroleum literature). In addition, all the layers are allowed to be anisotropic. In simulating water release due to water table decline in the manner of Neuman (1972) we assume that flow in the unsaturated zone above

the water table has negligible effect on flow in the saturated zone. Cooley (1971) solved the coupled saturated–unsaturated flow problem numerically, and recently, Tartakovsky and Neuman, 2007 have developed an approximate analytical solution to this saturated–unsaturated flow problem. For our purposes, the focus is on accounting for leakage in the unconfined aquifer flow problem, and the simulation of delayed water table response in the manner of Neuman (1972) is adopted for simplicity. It should be noted that Moench (1994) demonstrated that when the parameter estimation procedure is done correctly, it may be possible to obtain reasonable estimates of specific storage when water table response is modeled in the manner of Neuman (1972).

Our solution is more general than that developed by Zlotnik and Zhan (2005) as it allows for horizontal flow in the aquitard, and includes a confined aquifer below the aquitard. It can thus be used for modeling flow in aquifer–aquitard systems, where the radial component of flow in aquitards is significant. Zlotnik and Zhan (2005) concluded that leakage of water from the aquitard to the unconfined aquifer is negligible at late time. The results from the present work are at variance with these conclusions. Our solution predicts significant departure from the case with no leakage at both early-intermediate time and at late time. The model predicted results show low sensitivity to changes in radial hydraulic conductivities for aquitards that are two or more orders of magnitude smaller than those of the aquifers, in conformity to the findings of Neuman and Witherspoon (1969a). Hence, for cases where aquitard hydraulic conductivities are two or more orders of magnitude smaller than those of the aquifers, the simpler models that restrict flow to the radial direction in aquifers and to the vertical direction in aquitards may be sufficient. However, our solution predicts that one may obtain measurable differences in aquitard drawdown at different radial distances from the pumping well, indicating large radial hydraulic gradients can exist, even in cases where aquitard radial hydraulic conductivity is two orders of magnitude smaller than those of the aquifers. Though it is not rigorously demonstrated in this work, it seems plausible that the findings of Sepulveda (2008) that more accurate estimates of hydraulic parameter are obtainable when the more general flow pattern is assumed for the system, may be extended to the unconfined aquifer flow problem.

## Mathematical formulation of flow problem

We consider here coupled flow in a three-layer unconfined–confined aquifer system, where the aquifers are separated by an aquitard as shown in Fig. 1. To solve this flow problem, we adopt the following assumptions:

- (1) Flow in the unsaturated zone above the unconfined aquifer can be neglected (i.e. the water table is a moving material boundary).
- (2) Drawdown is significantly smaller than the initial saturated thickness of the aquifer (Neuman, 1972).
- (3) Flow is radially symmetric.
- (4) The confined aquifer is bounded from below by a no-flow boundary.

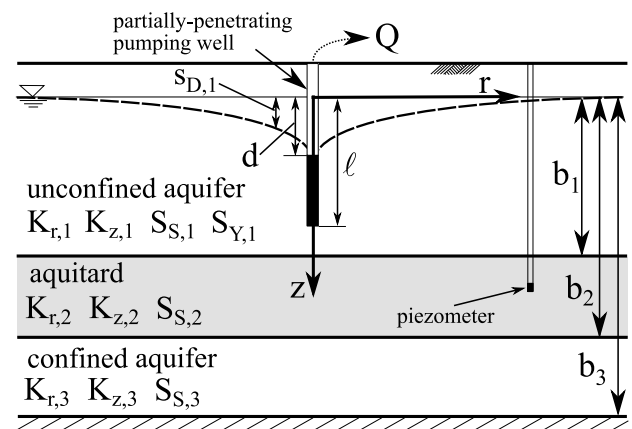


**Figure 1** Schematic of the three-layer system consisting of an unconfined aquifer, an aquitard, and a confined aquifer.

- (5) The aquifers and aquitard are homogeneous but anisotropic.
- (6) The coordinate axes are parallel to the principal directions of hydraulic conductivity.

Assumption (2) above is used to justify the application of the linearized kinematic boundary condition (see below) at the initial position of the water table as in Neuman (1972). The governing equation for flow in the aquifers and the aquitard is

$$S_{s,i} \frac{\partial s_i}{\partial t} = \frac{K_{r,i}}{r} \frac{\partial}{\partial r} \left( r \frac{\partial s_i}{\partial r} \right) + K_{z,i} \frac{\partial^2 s_i}{\partial z^2}, \quad (1)$$

where  $s_i$  is drawdown,  $S_{s,i}$  is specific storage,  $K_{r,i}$  and  $K_{z,i}$  are radial and vertical hydraulic conductivities, respectively,  $r, z, t$  are space-time coordinates, and  $i = 1, 2, 3$  for the unconfined aquifer, aquitard and confined aquifer, respectively. Eq. (1) is solved subject to the following initial and far-field boundary conditions for all  $i$

$$s_i(r, z, 0) = \lim_{r \rightarrow \infty} s_i(r, z, t) = 0. \quad (2)$$

In addition, for unconfined aquifer flow, Eq. (1) is solved subject to the following boundary conditions:

$$\lim_{r \rightarrow 0} r \frac{\partial s_1}{\partial r} = \begin{cases} 0 & \forall z \in (-d, 0], \\ -Q/[2\pi K_{r,1}(l-d)] & \forall z \in [-l, -d], \\ 0 & \forall z \in [-b_1, -l), \end{cases} \quad (3)$$

$$-K_{z,1} \frac{\partial s_1}{\partial z} \Big|_{z=0} = S_Y \frac{\partial s_1}{\partial t} \Big|_{z=0}, \quad (4)$$

where  $S_Y$  is the specific yield of the unconfined aquifer. For aquitard flow Eq. (1) is solved subject to the following boundary condition

$$\lim_{r \rightarrow 0} r \frac{\partial s_2}{\partial r} = 0 \quad (5)$$

and for confined aquifer flow

$$\lim_{r \rightarrow 0} r \frac{\partial s_3}{\partial r} = \frac{\partial s_3}{\partial z} \Big|_{z=-b_3} = 0. \quad (6)$$

At the common boundary between the unconfined aquifer and the aquitard ( $z = -b_1$ ), we apply the following continuity conditions:

$$s_1(r, -b_1, t) = s_2(r, -b_1, t), \quad (7)$$

$$K_{z,1} \frac{\partial s_1}{\partial z} \Big|_{z=-b_1} = K_{z,2} \frac{\partial s_2}{\partial z} \Big|_{z=-b_1}. \quad (8)$$

Similarly, at the common boundary between the aquitard and the confined aquifer ( $z = -b_2$ ), we apply the following continuity conditions:

$$s_2(r, -b_2, t) = s_3(r, -b_2, t), \quad (9)$$

$$K_{z,2} \frac{\partial s_2}{\partial z} \Big|_{z=-b_2} = K_{z,3} \frac{\partial s_3}{\partial z} \Big|_{z=-b_2}. \quad (10)$$

For convenience, Eq. (1) is expressed in dimensionless form as follows:

$$\frac{\partial s_{D,i}}{\partial t_D} = \frac{\alpha_{D,r}^{(i)}}{r_D} \frac{\partial}{\partial r_D} \left( r_D \frac{\partial s_{D,i}}{\partial r_D} \right) + \alpha_{D,z}^{(i)} \frac{\partial^2 s_{D,i}}{\partial z_D^2}, \quad (11)$$

where  $s_{D,i} = s_i/[Q/(4\pi K_{r,1} b_1)]$ ,  $t_D = \alpha_{r,1} t/b_1^2$ ,  $(r_D, z_D) = (r/b_1, z/b_1)$ ,  $\alpha_{D,r}^{(i)} = \alpha_{r,i}/\alpha_{r,1}$ ,  $\alpha_{D,z}^{(i)} = \alpha_{z,i}/\alpha_{r,1}$ ,  $\alpha_{r,i} = K_{r,i}/S_{s,i}$  and  $\alpha_{z,i} = K_{z,i}/S_{s,i}$ . A complete list of non-dimensional variables and parameters is given in Table 1. The initial and far-field boundary conditions in non-dimensional form become

$$s_{D,i}(r_D, z_D, 0) = \lim_{r_D \rightarrow \infty} s_{D,i}(r_D, z_D, t_D) = 0. \quad (12)$$

For the unconfined aquifer, the boundary conditions at the well ( $r_D = 0$ ) and the water table ( $z_D = 0$ ) become

$$\lim_{r_D \rightarrow 0} r_D \frac{\partial s_{D,1}}{\partial r_D} = \begin{cases} 0 & \forall z \in (-d_D, 0], \\ -2/(l_D - d_D) & \forall z \in [-l_D, -d_D], \\ 0 & \forall z \in [-1, -l_D], \end{cases} \quad (13)$$

$$-\frac{\partial s_{D,1}}{\partial z_D} \Big|_{z_D=0} = \frac{1}{\alpha_{D,Y}} \frac{\partial s_{D,1}}{\partial t_D} \Big|_{z_D=0}, \quad (14)$$

where  $\alpha_{D,Y} = \alpha_Y/\alpha_{r,1}$  and  $\alpha_Y = b_1 K_{z,1}/S_Y$ . For aquitard flow the boundary condition at  $r_D = 0$  becomes

$$\lim_{r_D \rightarrow 0} r_D \frac{\partial s_{D,2}}{\partial r_D} = 0 \quad (15)$$

and for confined aquifer flow, at  $r_D = 0$  and  $z_D = -b_{D,3}$  (confined aquifer base), we have

$$\lim_{r_D \rightarrow 0} r_D \frac{\partial s_{D,3}}{\partial r_D} = \frac{\partial s_{D,3}}{\partial z_D} \Big|_{z_D=-b_{D,3}} = 0. \quad (16)$$

The continuity conditions become

$$s_{D,1}(r_D, -1, t_D) = s_{D,2}(r_D, -1, t_D), \quad (17)$$

$$\frac{\partial s_{D,1}}{\partial z_D} \Big|_{z_D=-1} = \kappa_{z,2} \frac{\partial s_{D,2}}{\partial z_D} \Big|_{z_D=-1} \quad (18)$$

at the unconfined aquifer–aquitard boundary, where  $\kappa_{z,2} = K_{z,2}/K_{z,1}$ , and

$$s_{D,2}(r_D, -b_{D,2}, t_D) = s_{D,3}(r_D, -b_{D,2}, t_D), \quad (19)$$

$$\frac{\partial s_{D,2}}{\partial z_D} \Big|_{z_D=-b_{D,2}} = \kappa_{z,3} \frac{\partial s_{D,3}}{\partial z_D} \Big|_{z_D=-b_{D,2}} \quad (20)$$

at the confined aquifer–aquitard boundary, where  $\kappa_{z,3} = K_{z,3}/K_{z,2}$ .

## Exact solution in Laplace–Hankel transform space

The double Laplace–Hankel transform,  $\bar{s}_{D,1}^*$ , of drawdown response in the unconfined aquifer is given by (see Appendix A for details)

$$\bar{s}_{D,1}^*(a, z_D, p) = \bar{u}_D^*(a, z_D, p) + \bar{v}_D^*(a, z_D, p), \quad (21)$$

where  $a$  and  $p$  are the Hankel and Laplace transform variables, respectively,  $\bar{u}_D^*(a, z_D, p)$  is the double transform of drawdown in a confined aquifer due to pumping from a well of infinitesimal radius that partially penetrates the aquifer, and  $\bar{v}_D^*(a, z_D, p)$  accounts for water table and leakage boundary conditions. Thus,  $\bar{u}_D^*(a, z_D, p)$  corresponds to the double transform of the solution of Hantush (1964) for drawdown in a confined aquifer due to pumping from a well of infinitesimal radius that partially penetrates the aquifer. However, the representation of the solution given by Hantush (1964) involves an infinite sum that converges very slowly. An alternative representation of the Hantush solution in Laplace–Hankel transform space,  $\bar{u}_D^*$ , is

$$\bar{u}_D^*(a, z_D, p) = \frac{2[\cosh(\eta_1, \zeta_D) - \delta \bar{u}_D^*(\eta_1, z_D)]}{p \eta_1^2 \alpha_{D,z}^{(1)} (l_D - d_D)}, \quad (22)$$

where

$$\zeta_D = \begin{cases} d_D + z_D & \forall z_D \in (-d_D, 0], \\ 0 & \forall z_D \in [-l_D, -d_D], \\ l_D + z_D & \forall z_D \in [-1, -l_D] \end{cases} \quad (23)$$

and

$$\begin{aligned} \delta \bar{u}_D^*(\eta_1, z_D) &= \frac{\sinh(\eta_1 d_D) \cosh[\eta_1(1 + z_D)] + \sinh[\eta_1(1 - l_D)] \cosh(\eta_1 z_D)}{\sinh(\eta_1)}. \end{aligned} \quad (24)$$

The details of the derivation of the above solution are included in Appendix A. In the above equations and those to follow  $\eta_i = \sqrt{(p + \alpha_{D,r}^{(i)} a^2)/\alpha_{D,z}^{(i)}}$ , with  $i = 1, 2, 3$ . The values

**Table 1** Dimensionless variables and parameters

$s_{D,i} = s_i/[Q/(4\pi b_1 K_{r,1})]$
$z_D = z/b_1$
$r_D = r/b_1$
$t_D = \alpha_{r,1} t/b_1^2$
$b_{D,i} = b_i/b_1$
$d_D = d/b_1$
$l_D = l/b_1$
$\alpha_{D,r}^{(i)} = \alpha_{r,i}/\alpha_{r,1}$
$\alpha_{D,z}^{(i)} = \alpha_{z,i}/\alpha_{r,1}$
$\alpha_{D,Y} = \alpha_Y/\alpha_{r,1}$
$\eta_i = [(p + \alpha_{D,r}^{(i)} a^2)/\alpha_{D,z}^{(i)}]^{1/2}$
$\xi = \eta_1 \alpha_{D,Y}/p$
$\gamma_1 = \eta_2 \kappa_{z,2}/\eta_1$
$\gamma_2 = \eta_3 \kappa_{z,3}/\eta_2$
$\kappa_{z,i} = K_{z,i}/K_{z,i-1}$
$\theta_1 = \eta_3(b_{D,3} - b_{D,2}) + \eta_2(b_{D,2} - 1)$
$\theta_2 = \eta_3(b_{D,3} - b_{D,2}) - \eta_2(b_{D,2} - 1)$

of  $\bar{u}_D^*$  can be computed faster and more efficiently using Eq. (22) than using the Hantush (1964) representation.

It is shown in Appendix B that the component  $\bar{v}_D^*$  is given by

$$\bar{v}_D^*(a, z_D, p) = \bar{u}_{D,-1}^* \cosh[\eta_1(1 + z_D)] + \frac{f(\eta_1)h(a, z_D, p)}{\Delta}, \quad (25)$$

where  $u_{D,-1} = u_D(z_D = -1)$

$$\begin{aligned} h(a, z_D, p) = & \frac{(1 + \gamma_1)(1 + \gamma_2)}{2} \cosh[\eta_1(1 + z_D) + \theta_1] \\ & + \frac{(1 - \gamma_1)(1 + \gamma_2)}{2} \cosh[\eta_1(1 + z_D) - \theta_1] \\ & + \frac{(1 - \gamma_1)(1 - \gamma_2)}{2} \cosh[\eta_1(1 + z_D) + \theta_2] \\ & + \frac{(1 + \gamma_1)(1 - \gamma_2)}{2} \cosh[\eta_1(1 + z_D) - \theta_2], \quad (26) \end{aligned}$$

$\gamma_1 = \eta_2 \kappa_{z,2} / \eta_1$ ,  $\gamma_2 = \eta_3 \kappa_{z,3} / \eta_2$ ,  $\kappa_{z,i} = K_{z,i} / K_{z,i-1}$ ,  $\theta_1 = \eta_3(b_{D,3} - b_{D,2}) + \eta_2(b_{D,2} - 1)$ ,  $\theta_2 = \eta_3(b_{D,3} - b_{D,2}) - \eta_2(b_{D,2} - 1)$ , and the functions  $f(\eta_1)$  and  $\Delta$  are defined in Eqs. (B.18) and (B.21), respectively. For  $b_{D,2} = b_{D,3} = 0$ , that is for the case without the aquitard and lower aquifer and hence, no leakage, it can be shown that Eq. (25) reduces to

$$\bar{v}_D^* = -\frac{\bar{u}_{D,0}^* \cosh[\eta_1(1 + z_D)]}{\xi \sinh(\eta_1) + \cosh(\eta_1)}, \quad (27)$$

where  $\xi = \eta_1 \alpha_{D,Y} / p$  and  $u_{D,0} = u_D(z_D = 0)$ . Eq. (27) is the solution obtained that was obtained by Neuman (1974) for flow in a pumped unconfined aquifer without leakage.

It is also shown in Appendix B that the double Laplace–Hankel transform,  $\bar{s}_{D,2}^*(a, z_D, p)$ , of aquitard drawdown is given by

$$\begin{aligned} \bar{s}_{D,2}^*(a, z_D, p) = & -\frac{f(\eta_1)}{\Delta} \{(1 + \gamma_2) \cosh[\theta_1 + \eta_2(1 + z_D)] \\ & + (1 - \gamma_2) \cosh[\theta_2 - \eta_2(1 + z_D)]\}. \quad (28) \end{aligned}$$

The double Laplace–Hankel transform,  $\bar{s}_{D,3}^*(a, z_D, p)$ , of confined aquifer drawdown due to pumping in the unconfined aquifer is given by

$$\bar{s}_{D,3}^*(a, z_D, p) = \frac{-2f(\eta_1)}{\Delta} \cosh[\eta_3(b_{D,3} + z_D)]. \quad (29)$$

The exact analytical solutions obtained above for flow in the three layers were inverted numerically from the double transform space. In the next section the behavior predicted by these solutions is discussed.

## Numerical inversion of double Laplace–Hankel transform solutions

One can, in principle, obtain the analytical inverse Laplace transforms of  $\bar{s}_{D,1}^*$ ,  $\bar{s}_{D,2}^*$ , and  $\bar{s}_{D,3}^*$  by using the methods of complex contour integration, including the theory of residues (Neuman, 1972). In this work, however, the inverse Laplace and Hankel transforms are obtained numerically. The expressions for  $\bar{s}_{D,1}^*$ ,  $\bar{s}_{D,2}^*$  and  $\bar{s}_{D,3}^*$  were evaluated in Laplace–Hankel space using extended precision (greater than Fortran double precision). Extended precision is used to handle the ratios of exponentially growing components of the hyperbolic trigonometric functions. Different exponentially-growing terms would need to be factored out at early time, compared to late time; such terms are also

strongly dependent on position  $(r_D, z_D)$ . Working in extended precision is, in a sense, the “brute force” approach of ensuring numerical computations are bounded, as loss of numerical significance (due to subtraction of nearly equivalent values) leads to early- and late time exponential blow-up. It allows one to avoid the need to develop special-case double-precision solutions for every possible combination of parameters.

The inverse Laplace transform was obtained first using the doubly-accelerated Fourier series approach of de Hoog et al. (1982). The inverse Hankel transform (see Appendix A) was approximated by splitting the improper Hankel integral into a finite integral over the interval  $0 \leq a \leq j_{0,n}$ , and an infinite integral over the interval  $j_{0,n} \leq a < \infty$ , in a manner similar to that proposed by Wieder (1999). The integral is split at  $j_{0,n}$ , the  $n$ th zero of  $J_0(ar_D)$ . The finite portion of the integral was evaluated using the QXGS automatic integration routine (Favati et al., 1991). Most of the contribution to the total Hankel integral comes from the finite portion of this integral. The infinite integral was approximated by integrating between each  $j_{0,n}$  and  $j_{0,n+1}$ , as  $n$  becomes large, using Gauss–Lobatto quadrature for each interval. Finally, partial sums of the areas (which alternate in sign) were accelerated with Wynn’s  $\epsilon$ -algorithm (Antia, 2002). Because of the decaying magnitude and alternating signs of the areas between successive zeros, the  $\epsilon$ -algorithm was very effective.

## Model predicted behavior

In the figures shown here,  $E_1(\cdot)$  represents the exponential integral (Theis solution),  $x = r_D^2 / 4t_D$  and  $x_Y = r_D^2 / 4t_{D,Y}$ , where  $t_{D,Y} = \alpha_Y t / b_Y^2$  and  $\alpha_Y = b_Y K_{z,1} / S_Y$ . Figs. 2 and 3 show the variation of drawdown with dimensionless time for different values of depth and radial distance, respectively, for (a) a fully and (b) a partially ( $d_D = 0.5$ ,  $l_D = 1.0$ ) penetrating pumping well. It should be noted that  $z_D = 0$  is at the initial position of the water table and  $z_D = -1.0$  corresponds to bottom boundary of the unconfined aquifer. The results shown in Fig. 2 were computed at  $r_D = 0.5$ , whereas those shown in Fig. 3 were computed at  $z_D = -0.9$ , near the base of the unconfined aquifer. The dimensionless parameter values used in computing the results are  $\alpha_{D,Y} = 2.4 \times 10^{-3}$ ,  $\alpha_{D,r}^{(2)} = \alpha_{D,z}^{(2)} = 1.0 \times 10^{-3}$ ,  $\alpha_{D,r}^{(3)} = \alpha_{D,z}^{(3)} = 1.0$ ,  $\kappa_{z,2} = 0.02$  and  $\kappa_{z,3} = 50$ . The results show that leakage can lead to significant deviation of model predicted drawdown from that predicted by the solution in which leakage is not accounted for. This deviation is seen at both early and late time in both cases (partial and full penetration of pumping well).

In particular, results in Fig. 2 show that at early time, for both partial and full penetration, the effect of leakage decreases with increasing vertical distance from the common boundary between the unconfined aquifer and the aquitard. In fact, for  $z_D \geq -0.5$ , the early time response of the case with leakage is virtually indistinguishable from that with leakage, while at intermediate and late times, the effect of leakage persists at all vertical distances from the unconfined aquifer–aquitard boundary. Results in Fig. 3 indicate that the effect of leakage on unconfined aquifer response recorded by piezometers close to the unconfined aquifer–aquitard boundary is significant at all radial distances from the pumping well at all times.

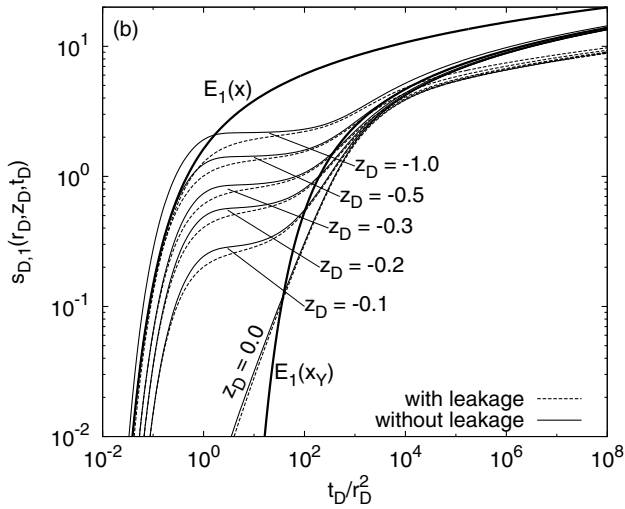
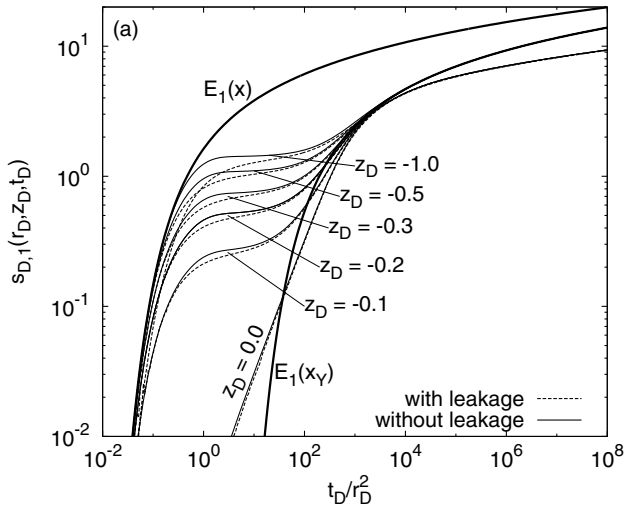


**Figure 2** Log–log plot of unconfined aquifer dimensionless drawdown,  $s_{D,1}$ , against  $t_D/r_D^2$  at  $r_D = 0.5$  for different values of  $z_D$ . Results are for (a) a fully penetrating and (b) partially penetrating pumping well.

Fig. 4 shows the effect of the dimensionless vertical hydraulic conductivity of the aquitard,  $\kappa_{z,2}$ , on drawdown response in the unconfined aquifer with leakage for the case of a partially penetrating pumping well. In Fig. 4 the radial hydraulic of the aquitard was fixed at  $K_{r,2} = 6 \times 10^{-6}$  m/s, the pumping well was screened over the interval  $[-0.5, -1.0]$ , and  $\kappa_{z,3} = 50$ . The other dimensionless parameter values used in computing the results were  $\alpha_{D,y} = 2.4 \times 10^{-3}$ ,  $\alpha_{D,r}^{(2)} = 1.0 \times 10^{-3}$ ,  $\alpha_{D,z}^{(3)} = \alpha_{D,z}^{(3)} = 1.0$ . The results in the figure, computed at  $(r_D, z_D) = (0.8, -0.9)$ , indicate that the vertical hydraulic conductivity of the aquitard has a strong effect on the response of the unconfined aquifer at all times because vertical flow in the aquitard is significant at all times; it is the primary direction of water flow from the aquitard to the pumping well.

The effect of the radial conductivity of the aquitard,  $K_{r,2}$ , on unconfined aquifer response to pumping from a partially pumping well is shown in Fig. 5 for the case with  $\kappa_{z,2} = 5 \times 10^{-2}$ ,  $b_{D,2} = 1.5$  and  $b_{D,3} = 2.5$ . The results in the figure, computed at  $(r_D, z_D) = (0.5, -1.0)$ , show that the ef-

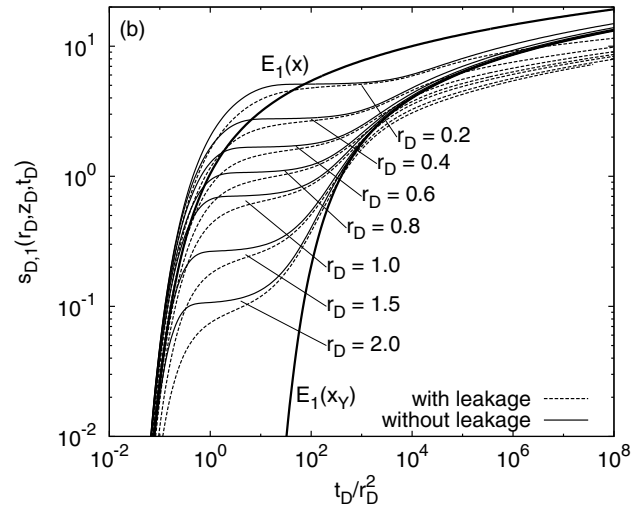
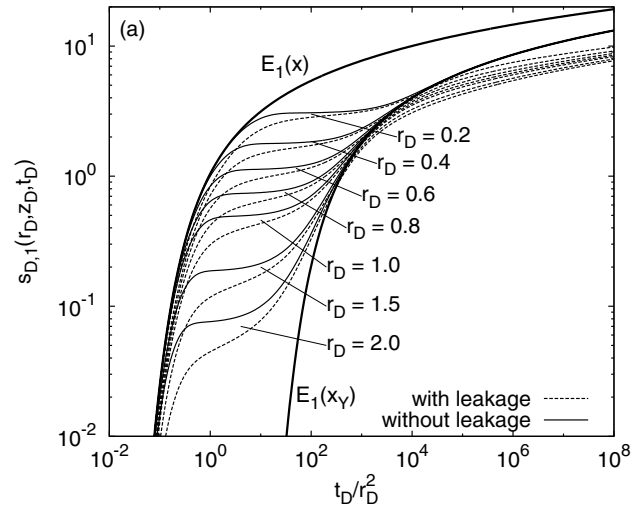


**Figure 3** Log–log plot of unconfined aquifer dimensionless drawdown,  $s_{D,1}$ , against  $t_D/r_D^2$  at  $z_D = -0.9$  for different values of  $r_D$ . Results are for (a) a fully penetrating and (b) partially penetrating pumping well.

fect of changing  $K_{r,2}$  is negligible at early time but can be significant at late time, if  $K_{r,2}$  is significantly greater than  $\kappa_{z,2}$ . This is due to the fact that, at early time water is withdrawn from elastic storage close to the pumping well and is predominantly vertical in the aquitard. At late time, water is conveyed to the pumping well from further radial distances in the aquitard, hence the aquitard horizontal hydraulic conductivity becomes important. Additionally, it should be noted that for water-deposited sedimentary formations, the horizontal hydraulic conductivity is typically greater than the vertical. Hence, flow models that neglect horizontal flow in the aquitard may lead to significant error in predicted unconfined aquifer response to pumping.

Fig. 6 is a plot of the dimensionless aquitard drawdown,  $s_{D,2}$ , against  $t_D$  for different radial distances from the pumping well at (a)  $z_D = -1.05$  and (b)  $z_D = -1.25$ . The following dimensionless parameters were used in computing these results  $\kappa_{z,2} = 0.10$ ,  $\kappa_{z,3} = 5.0$ ,  $\alpha_{D,r}^{(2)} = \alpha_{D,z}^{(2)} = 5 \times 10^{-4}$  and  $\alpha_{D,r}^{(3)} = \alpha_{D,z}^{(3)} = 2.5 \times 10^{-1}$ . The thicknesses of layers  $i = 1, 2, 3$  were 20, 30 and 100 m, respectively. Hence, the results

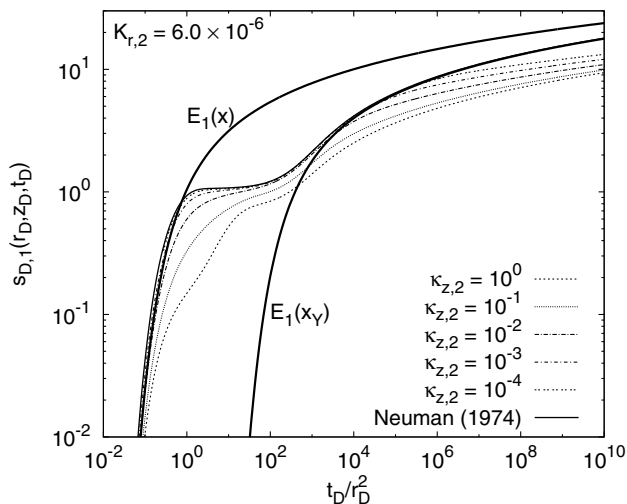


**Figure 4** Log–log plot of unconfined aquifer dimensionless drawdown,  $s_{D,1}$ , against  $t_D/r_D^2$  at  $(r_D, z_D) = (0.8, -0.9)$  for different values of  $\kappa_{z,2}$  with  $K_{r,2} = 6 \times 10^{-6}$ .

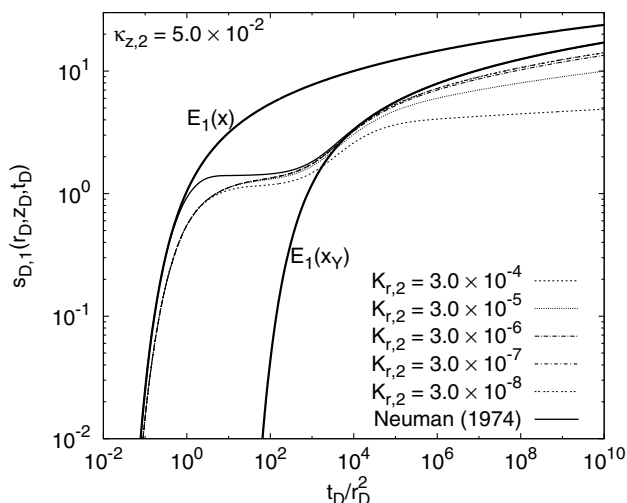


**Figure 5** Log–log plot of unconfined aquifer dimensionless drawdown,  $s_{D,1}$ , against,  $t_D/r_D^2$  at  $(r_D, z_D) = (0.5, -1.0)$  for different values of  $K_{r,2}$ , with  $\kappa_{z,2} = 5 \times 10^{-2}$  and  $\kappa_{z,3} = 20$ .

shown in Fig. 6a were computed in the aquitard at 1 m below the unconfined aquifer and those in (b) at 5 m below the unconfined aquifer. The results show that drawdown in the aquitard is a strong function of the radial distance from the pumping well even 5 m into the aquitard, which is contrary to the assumptions of entirely vertical flow in the aquitard adopted by Zlotnik and Zhan (2005). In fact, even when the vertical and radial hydraulic conductivities of the aquitard are reduced by an order of magnitude, such that  $\kappa_{z,2} = 0.01$  and  $\kappa_{z,3} = 50.0$ , the variation of  $s_{D,2}$  with  $r_D$  is still significant as indicated by the results plotted in Fig. 7.

Fig. 8 shows a log–log plot of dimensionless aquitard drawdown,  $s_{D,2}$ , against  $t_D/r_D^2$  at  $r_D = 0.5$ , for different values of  $z_D$ . The dimensionless parameters used to compute the results are (a)  $\kappa_{z,2} = 0.10$ ,  $\kappa_{z,3} = 5.0$ ,  $\alpha_{D,r}^{(2)} = \alpha_{D,z}^{(2)} = 5 \times 10^{-4}$  and  $\alpha_{D,r}^{(3)} = \alpha_{D,z}^{(3)} = 2.5 \times 10^{-1}$  and (b)  $\kappa_{z,2} = 0.01$ ,  $\kappa_{z,3} = 50.0$ ,  $\alpha_{D,r}^{(2)} = \alpha_{D,z}^{(2)} = 5 \times 10^{-5}$  and  $\alpha_{D,r}^{(3)} = \alpha_{D,z}^{(3)} = 2.5 \times$

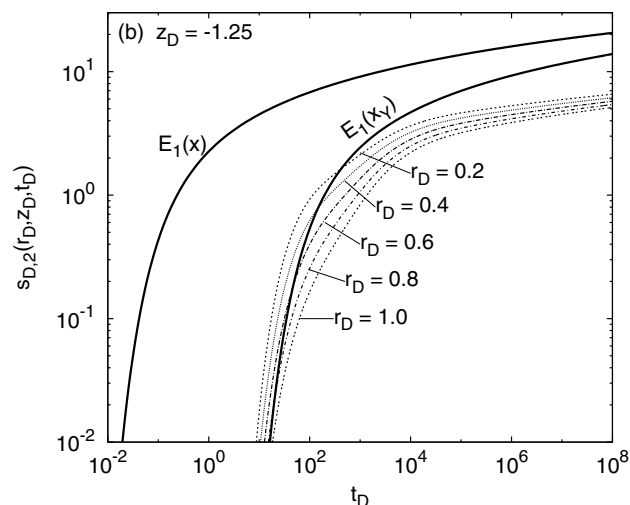
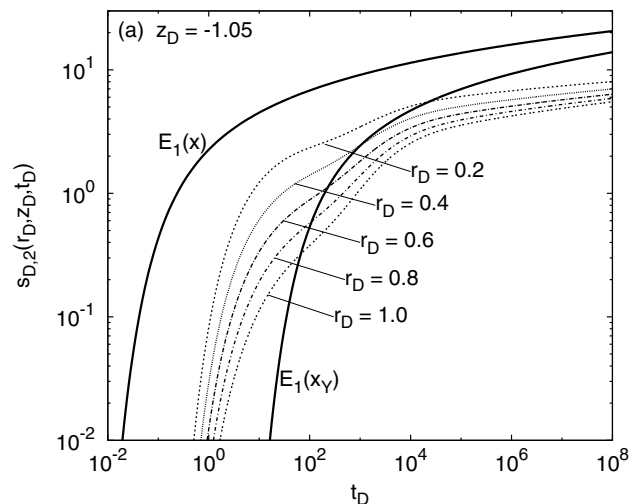


**Figure 6** Log–log plot of aquitard dimensionless drawdown,  $s_{D,2}$ , against  $t_D$  for different values of  $r_D$  at  $z_D = -1.05$  and (b)  $z_D = -1.25$ .

$10^{-1}$ . As would be expected, drawdown in the aquitard decreases with increasing vertical distance from the unconfined aquifer–aquitard boundary. The effect of the water table also diminishes with increasing distance from this boundary. The inflection attributable to water table decline vanishes with increasing depth into the aquitard. It vanishes more rapidly with depth for smaller values of  $\kappa_{z,2}$ , which correspond to increasingly less conductive aquitards relative to the unconfined aquifer.

Using the parameter values  $\kappa_{z,2} = 0.1$ ,  $\kappa_{z,3} = 5.0$ ,  $\alpha_{D,r}^{(2)} = \alpha_{D,z}^{(2)} = 5 \times 10^{-5}$  and  $\alpha_{D,r}^{(3)} = \alpha_{D,z}^{(3)} = 2.5 \times 10^{-1}$ , we investigated the effect of aquitard and confined aquifer thickness on the unconfined aquifer response to pumping. The results are shown in Fig. 9 at  $z_D = -1.0$ , where  $b_{D,2}^* = b_{D,2} - 1$  and  $b_{D,3}^* = b_{D,3} - b_{D,2}$  are the dimensionless thicknesses of the aquitard and confined aquifer, respectively. In Fig. 9a,  $b_{D,3}^*$  was fixed at 0.5 while  $b_{D,2}^*$  was varied, where as in (b), we set  $b_{D,2}^* = 0.5$  and varied  $b_{D,3}^*$ . The results show that even for a relatively thin aquitard (e.g.  $b_{D,2}^* = 0.1$ ) drawdown in the unconfined aquifer shows significant deviation from the Neuman (1972) solution (no leakage). Increasing the

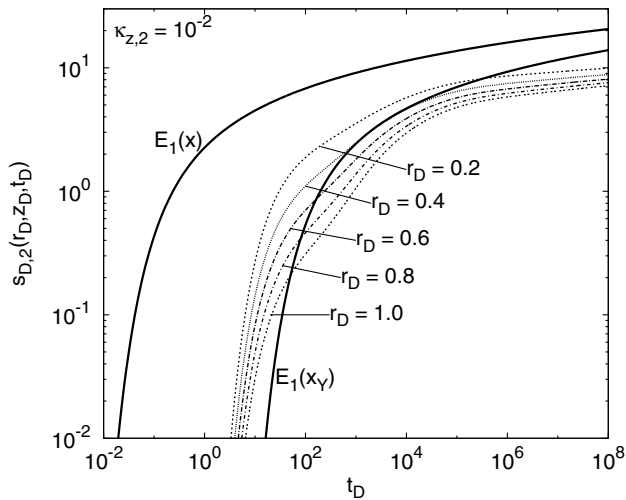


**Figure 7** Log–log plot of aquitard dimensionless drawdown,  $s_{D,2}$ , against  $t_D$  for different values of  $r_D$  at  $z_D = -1.05$  for  $\kappa_{z,2} = 0.01$  and  $\kappa_{z,2} = 50.0$ .

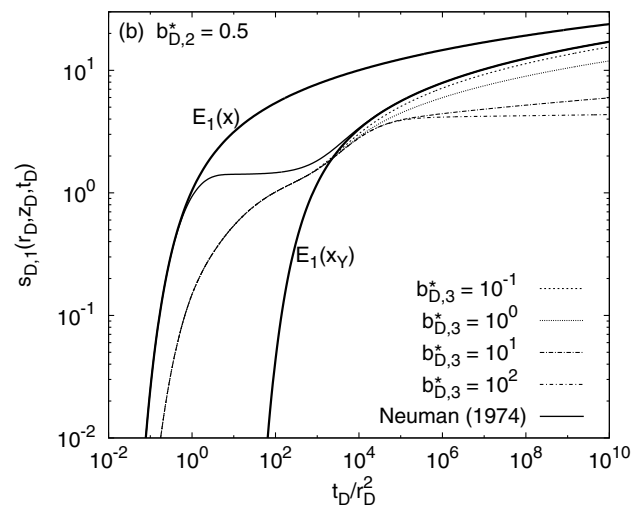
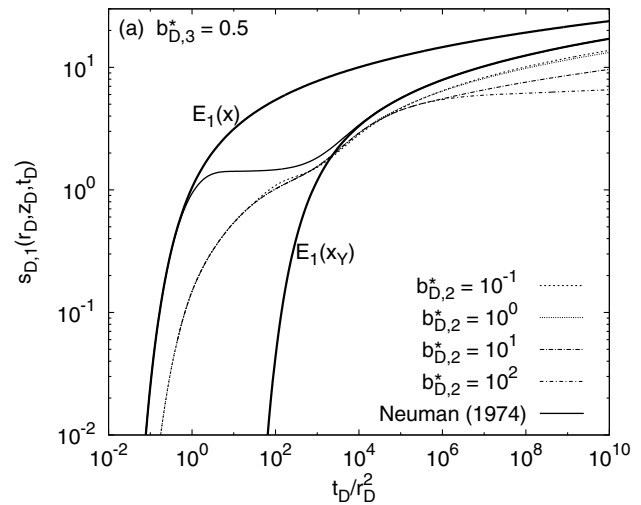


**Figure 9** Log–log plot of unconfined aquifer dimensionless drawdown,  $s_{D,1}$ , against  $t_D/r_D^2$  at  $(r_D, z_D) = (0.5, -1.0)$  for different values of (a)  $b_{D,2}^* = b_{D,2} - 1.0$ , the dimensionless aquitard thickness and (b)  $b_{D,3}^* = b_{D,3} - b_{D,2}$ , the dimensionless confined aquifer thickness.

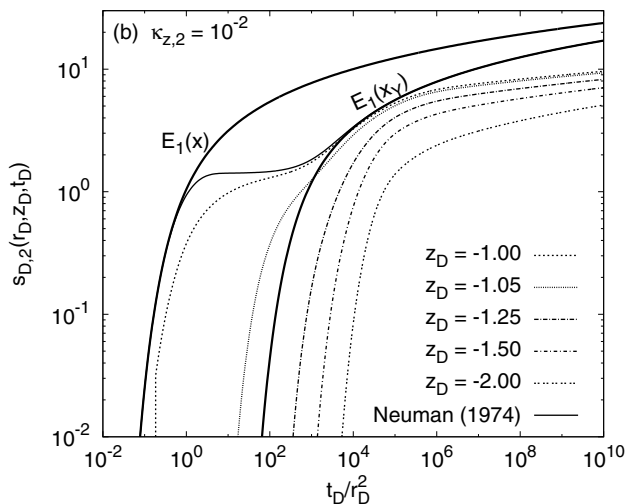
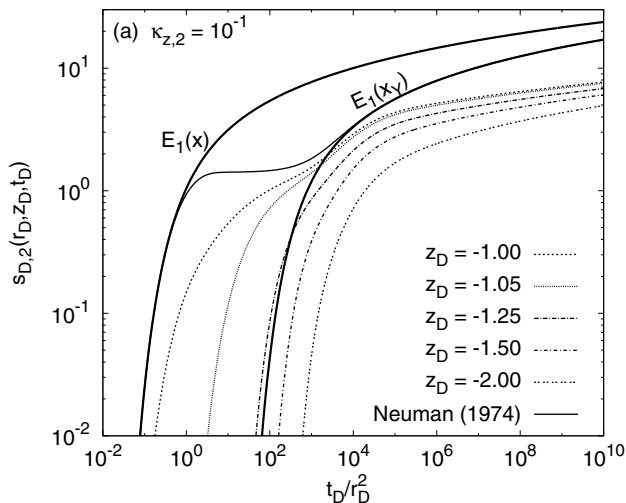


**Figure 8** Log–log plot of dimensionless aquitard drawdown,  $s_{D,2}$ , against  $t_D/r_D^2$ , at  $r_D = 0.5$  for different values of  $z_D$ . Plot in (a) is for  $\kappa_{z,2} = 0.1$  and (b) is for  $\kappa_{z,2} = 0.01$ .

thickness of the aquitard affects only the late time drawdown response of the unconfined aquifer. This is attributed to the fact that at late time water has to be withdrawn from a region of influence that is sensitive to aquitard thickness, whereas at early time, water is primarily withdrawn from elastic storage in the immediate vicinity of the pumping well. Increasing the confined aquifer thickness has the same effect. The major difference is that there is greater sensitivity of the late time unconfined aquifer response to changing confined aquifer thickness than to changing aquitard thickness. In both case, in the limit as  $b_{D,2}^* \rightarrow \infty$  or  $b_{D,3}^* \rightarrow \infty$ , predicted unconfined aquifer response approaches a steady-state as the lower layers become infinite sources of water.

### Summary

The solution presented here incorporates the effects of leakage into the solution for flow in unconfined aquifer toward a partially penetrating pumping well. In this solution

horizontal flow in the aquitard and vertical flow in the confined aquifer were not neglected and unconfined aquifer flow was treated in the manner of Neuman (1972). We used drawdown and flux continuity conditions at the two contacts between the three layers, removing the need to make the assumptions adopted in the classical and modified leakage theories of Hantush and Jacob (1955) and Hantush (1960).

The solution presented here is more general than similar solutions obtained for the problem of leakage in confined systems, as it is not restricted to cases of strictly horizontal flow in the confined aquifer and strictly vertical flow in the aquitard. The behavior of the system predicted by this solution shows significant departure from the solution of Neuman (1974), which does not account for leakage at the base of the unconfined aquifer. Such deviation is seen at both early and late times, which is at variance with the results of Ehlig and Halepaska (1976) that showed departure only at late time. Our solution is more general than that developed by Zlotnik and Zhan (2005) as it allows for horizontal flow in the aquitard and, and includes a confined aquifer below the aquitard. Zlotnik and Zhan (2005) concluded that leakage of water from the aquitard to the unconfined aquifer plays a minor role often at short and intermediate times. At large times, the role of the leakage was deemed negligible. The results from the present work are at variance with these conclusions. Our solution predicts significant departure from the case with no leakage at both early-intermediate time and at late time. Depending on parameter choices, predicted unconfined aquifer response may even approach a steady-state at late time.

The results presented here also indicate that sensitivity to the radial hydraulic conductivity of the aquitard is low if aquitard conductivities are two or more orders of magnitude smaller than those of the aquifers. This conforms to finding of Neuman and Witherspoon (1969a) who stated that "when the permeabilities of the aquifers are two or more orders of magnitude greater than that of the aquitard, errors introduced by this assumption are usually less than 5%". However, our solution predicts that one may obtain measurable differences in aquitard drawdown at different radial distances from the pumping well, producing large radial hydraulic gradients in the aquitard.

It is typically the case that the inverse Laplace transform is obtained analytically whereas the inverse Hankel transform is obtained numerically (Neuman, 1972; Neuman, 1974). In this work, both inverse transforms are obtained numerically. Given the widespread availability of efficient parameter estimation codes, the solution developed here can be useful for estimating unconfined aquifer, aquitard and confined aquifer hydraulic parameters. This can be accomplished through solution of an inverse problem using parameter estimation codes, such as PEST (Doherty, 2002).

## Acknowledgements

The work presented here was supported, in part, by EPA Grant X-960041-01-0. We would like to thank Dr. Henk Haitjema and an anonymous reviewer for their detailed review and insightful comments, corrections and recommendations

that lead to considerable improvement in the work presented here.

## Appendix A

Drawdown,  $s_{D,1}$ , in the unconfined aquifer can be decomposed as  $s_{D,1} = u_D + v_D$ , where  $u_D$  solves

$$\frac{\partial u_D}{\partial t_D} = \frac{1}{r_D} \frac{\partial}{\partial r_D} \left( r_D \frac{\partial u_D}{\partial r_D} \right) + \alpha_{D,z}^{(1)} \frac{\partial^2 u_D}{\partial z_D^2}, \quad (\text{A.1})$$

$$u_D(r_D, z_D, 0) = \lim_{r_D \rightarrow \infty} u_D(r_D, z_D, t_D) = 0, \quad (\text{A.2})$$

$$\lim_{r_D \rightarrow 0} r_D \frac{\partial u_D}{\partial r_D} = \begin{cases} 0 & \forall z_D \in (-d_D, 0], \\ -2/(l_D - d_D) & \forall z_D \in [-l_D, -d_D], \\ 0 & \forall z_D \in [-1, -l_D], \end{cases} \quad (\text{A.3})$$

$$\left. \frac{\partial u_D}{\partial z_D} \right|_{z_D=0} = \left. \frac{\partial u_D}{\partial z_D} \right|_{z_D=-1} = 0 \quad (\text{A.4})$$

and  $v_D$  solves

$$\frac{\partial v_D}{\partial t_D} = \frac{1}{r_D} \frac{\partial}{\partial r_D} \left( r_D \frac{\partial v_D}{\partial r_D} \right) + \alpha_{D,z}^{(1)} \frac{\partial^2 v_D}{\partial z_D^2}, \quad (\text{A.5})$$

$$v_D(r_D, z_D, 0) = \lim_{r_D \rightarrow \infty} v_D(r_D, z_D, t_D) = 0, \quad (\text{A.6})$$

$$\lim_{r_D \rightarrow 0} r_D \frac{\partial v_D}{\partial r_D} = 0, \quad (\text{A.7})$$

$$-\left. \frac{\partial v_D}{\partial z_D} \right|_{z_D=0} = \frac{1}{\alpha_{D,y}} \left( \left. \frac{\partial u_D}{\partial t_D} \right|_{z_D=0} + \left. \frac{\partial v_D}{\partial t_D} \right|_{z_D=0} \right). \quad (\text{A.8})$$

Applying the double Laplace–Hankel transform to Eq. (A.1) and simplifying subject to the initial condition leads to

$$\frac{d^2 \bar{u}_D^*}{dz_D^2} - \eta_1^2 \bar{u}_D^* = \frac{1}{\alpha_{D,z}^{(1)}} \lim_{r_D \rightarrow 0} r_D \frac{\partial \bar{u}_D}{\partial r_D}, \quad (\text{A.9})$$

which is solved subject to

$$\lim_{r_D \rightarrow 0} r_D \frac{\partial \bar{u}_D}{\partial r_D} = \begin{cases} 0 & \forall z_D \in (-d_D, 0], \\ -2/[p(l_D - d_D)] & \forall z_D \in [-l_D, -d_D], \\ 0 & \forall z_D \in [-1, -l_D], \end{cases} \quad (\text{A.10})$$

$$\left. \frac{d\bar{u}_D^*}{dz_D} \right|_{z_D=0} = \left. \frac{d\bar{u}_D^*}{dz_D} \right|_{z_D=-1} = 0. \quad (\text{A.11})$$

The general solutions to Eq. (A.9) are

$$\bar{u}_D^* = A_1 e^{\eta_1 z_D} + B_1 e^{-\eta_1 z_D}, \quad z \in (-d_D, 0], \quad (\text{A.12})$$

$$\bar{u}_D^* = A_2 e^{\eta_1 z_D} + B_2 e^{-\eta_1 z_D}, \quad z \in [-1, -l_D] \quad (\text{A.13})$$

and

$$\bar{u}_D^* = A_3 e^{\eta_1 z_D} + B_3 e^{-\eta_1 z_D} + \frac{2}{p\eta_1^2 \alpha_{D,z}^{(1)} (l_D - d_D)} \quad z \in [-l_D, -d_D]. \quad (\text{A.14})$$

Applying the boundary condition at  $z_D = 0$  to Eq. (A.12) yields

$$A_1 = B_1. \quad (\text{A.15})$$

Applying the boundary condition at  $z_D = -1$  to Eq. (A.13) yields

$$A_2 e^{-\eta_1} - B_2 e^{\eta_1} = 0. \quad (\text{A.16})$$

Enforcing continuity of  $\bar{u}_D^*$  and its first derivative at  $z_D = -d_D$  and  $z_D = -l_D$  leads to

$$(A_1 - A_3) e^{-\eta_1 d_D} + (B_1 - B_3) e^{\eta_1 d_D} = 2/[p\eta_1^2 \alpha_{D,z}^{(1)}(l_D - d_D)], \quad (\text{A.17})$$

$$(A_1 - A_3) e^{-\eta_1 l_D} - (B_1 - B_3) e^{\eta_1 l_D} = 0, \quad (\text{A.18})$$

$$(A_2 - A_3) e^{-\eta_1 l_D} + (B_2 - B_3) e^{\eta_1 l_D} = 2/[p\eta_1^2 \alpha_{D,z}^{(1)}(l_D - d_D)], \quad (\text{A.19})$$

$$(A_2 - A_3) e^{-\eta_1 l_D} - (B_2 - B_3) e^{\eta_1 l_D} = 0. \quad (\text{A.20})$$

Solving Eqs. (A.15)–(A.20) for the constants (in  $z_D$ ) leads to

$$A_1 = B_1 = \frac{e^{\eta_1 d_D} - \bar{w}_{D,1}^*(\eta_1)}{p\eta_1^2 \alpha_{D,z}^{(1)}(l_D - d_D)} = \frac{e^{-\eta_1 d_D} - \bar{w}_{D,2}^*(\eta_1)}{p\eta_1^2 \alpha_{D,z}^{(1)}(l_D - d_D)}, \quad (\text{A.21})$$

$$A_2 = \frac{e^{\eta_1 l_D} - \bar{w}_{D,1}^*(\eta_1)}{p\eta_1^2 \alpha_{D,z}^{(1)}(l_D - d_D)}, \quad (\text{A.22})$$

$$B_2 = \frac{e^{-\eta_1 l_D} - \bar{w}_{D,2}^*(\eta_1)}{p\eta_1^2 \alpha_{D,z}^{(1)}(l_D - d_D)}, \quad (\text{A.23})$$

$$A_3 = -\frac{\bar{w}_{D,1}^*(\eta_1)}{p\eta_1^2 \alpha_{D,z}^{(1)}(l_D - d_D)}, \quad (\text{A.24})$$

$$B_3 = -\frac{\bar{w}_{D,2}^*(\eta_1)}{p\eta_1^2 \alpha_{D,z}^{(1)}(l_D - d_D)}, \quad (\text{A.25})$$

where

$$\bar{w}_{D,1}^*(\eta_1) = \frac{e^{\eta_1} \sinh(\eta_1 d_D) + \sinh[\eta_1(1 - l_D)]}{\sinh(\eta_1)} \quad (\text{A.26})$$

and

$$\bar{w}_{D,2}^*(\eta_1) = \frac{e^{-\eta_1} \sinh(\eta_1 d_D) + \sinh[\eta_1(1 - l_D)]}{\sinh(\eta_1)}. \quad (\text{A.27})$$

Substituting these expressions for the constants into Eqs. (A.12)–(A.14) and simplifying leads to Eq. (22).

## Appendix B

Applying the double Laplace–Hankel transform to Eq. (A.5) and simplifying subject to the initial and boundary conditions given in Eqs. (A.6) and (A.7) leads to

$$\frac{d^2 \bar{v}_D^*}{dz_D^2} - \eta_1^2 \bar{v}_D^* = 0. \quad (\text{B.1})$$

The general solution to Eq. (B.1) is

$$\bar{v}_D^*(\eta_1, z_D) = c_1 e^{\eta_1 z_D} + c_2 e^{-\eta_1 z_D}. \quad (\text{B.2})$$

Applying the boundary condition at the water table given by Eqs. (A.8)–(A.27), (B.1), (B.2) leads to

$$-(\xi + 1)c_1 + (\xi - 1)c_2 = \bar{u}_D^*(\eta_1, z_D = 0). \quad (\text{B.3})$$

Applying the double Laplace–Hankel transform to Eq. (11) and simplifying subject to the initial and boundary conditions given in Eqs. (12) and (15) leads to

$$\frac{d^2 \bar{s}_{D,2}^*}{dz_D^2} - \eta_2^2 \bar{s}_{D,2}^* = 0, \quad (\text{B.4})$$

which has the following general solution:

$$\bar{s}_{D,2}^*(\eta_2, z_D) = c_3 e^{\eta_2 z_D} + c_4 e^{-\eta_2 z_D}. \quad (\text{B.5})$$

Applying the continuity conditions at  $z_D = -1$  leads to

$$-c_1 e^{-\eta_1} - c_2 e^{\eta_1} + c_3 e^{-\eta_2} + c_4 e^{\eta_2} = \bar{u}_D^*(\eta_1, z_D = -1) \quad (\text{B.6})$$

and

$$c_1 e^{-\eta_1} - c_2 e^{\eta_1} - c_3 \gamma_1 e^{-\eta_2} + c_4 \gamma_1 e^{\eta_2} = 0. \quad (\text{B.7})$$

Similarly, the general solution for the double Laplace–Hankel transform of confined aquifer drawdown,  $\bar{s}_{D,3}^*$  is

$$\bar{s}_{D,3}^*(\eta_3, z_D) = c_5 e^{\eta_3 z_D} + c_6 e^{-\eta_3 z_D}. \quad (\text{B.8})$$

Applying the no-flow boundary condition at  $z_D = -b_{D,3}$  leads to

$$c_5 e^{-\eta_3 b_{D,3}} - c_6 e^{\eta_3 b_{D,3}} = 0, \quad (\text{B.9})$$

whereas applying continuity conditions at  $z_D = -b_{D,2}$  leads to

$$c_3 e^{-\eta_2 b_{D,2}} + c_4 e^{\eta_2 b_{D,2}} - c_5 e^{-\eta_3 b_{D,2}} - c_6 e^{\eta_3 b_{D,2}} = 0 \quad (\text{B.10})$$

and

$$c_3 e^{-\eta_2 b_{D,2}} - c_4 e^{\eta_2 b_{D,2}} - c_5 \gamma_2 e^{-\eta_3 b_{D,2}} + c_6 \gamma_2 e^{\eta_3 b_{D,2}} = 0. \quad (\text{B.11})$$

Eqs. (B.3), (B.6), (B.7), (B.9)–(B.11) constitute a linear system of equations in six unknowns. Solving this system for  $c_1$ – $c_6$  yields

$$c_3 = -\frac{e^{\eta_2 b_{D,2}} f(\eta_1) g_2(\eta_2, \eta_3)}{\Delta} \quad (\text{B.12})$$

and

$$c_4 = -\frac{e^{-\eta_2 b_{D,2}} f(\eta_1) g_1(\eta_2, \eta_3)}{\Delta} \quad (\text{B.13})$$

with  $c_1, c_2, c_5$  and  $c_6$  expressed in terms of  $c_3$  and  $c_4$  as

$$c_1 = -\frac{1}{2} e^{\eta_1} [\bar{u}_{D,-1}^* - c_3(1 + \gamma_1) e^{-\eta_2} - c_4(1 - \gamma_1) e^{\eta_2}], \quad (\text{B.14})$$

$$c_2 = -\frac{1}{2} e^{-\eta_1} [\bar{u}_{D,-1}^* - c_3(1 - \gamma_1) e^{-\eta_2} - c_4(1 + \gamma_1) e^{\eta_2}], \quad (\text{B.15})$$

$$c_5 = \frac{1}{2} e^{\eta_3 b_{D,2}} [c_3(1 + 1/\gamma_2) e^{-\eta_2 b_{D,2}} + c_4(1 - 1/\gamma_2) e^{\eta_2 b_{D,2}}], \quad (\text{B.16})$$

$$c_6 = \frac{1}{2} e^{-\eta_3 b_{D,2}} [c_3(1 - 1/\gamma_2) e^{-\eta_2 b_{D,2}} + c_4(1 + 1/\gamma_2) e^{\eta_2 b_{D,2}}], \quad (\text{B.17})$$

where

$$f(\eta_1) = \bar{u}_{D,0}^* - \bar{u}_{D,-1}^* [\xi \sinh(\eta_1) + \cosh(\eta_1)], \quad (\text{B.18})$$

$$g_1(\eta_2, \eta_3) = \cosh[\eta_3(b_{D,3} - b_{D,2})] - \gamma_2 \sinh[\eta_3(b_{D,3} - b_{D,2})], \quad (\text{B.19})$$

$$g_2(\eta_2, \eta_3) = \cosh[\eta_3(b_{D,3} - b_{D,2})] + \gamma_2 \sinh[\eta_3(b_{D,3} - b_{D,2})], \quad (\text{B.20})$$

$$\begin{aligned} \Delta = & \frac{(1 + \gamma_1)(1 + \gamma_2)}{2} [\xi \sinh(\eta_1 + \theta_1) + \cosh(\eta_1 + \theta_1)] \\ & + \frac{(1 - \gamma_1)(1 + \gamma_2)}{2} [\xi \sinh(\eta_1 - \theta_1) + \cosh(\eta_1 - \theta_1)] \\ & + \frac{(1 - \gamma_1)(1 - \gamma_2)}{2} [\xi \sinh(\eta_1 + \theta_2) + \cosh(\eta_1 + \theta_2)] \\ & + \frac{(1 + \gamma_1)(1 - \gamma_2)}{2} [\xi \sinh(\eta_1 - \theta_2) + \cosh(\eta_1 - \theta_2)] \end{aligned} \quad (\text{B.21})$$

with  $\bar{u}_{D,0}^* = \bar{u}_D^*(a, z_D = 0, p)$  and  $\bar{u}_{D,1}^* = \bar{u}_D^*(a, z_D = -1, p)$ . Substituting the above expressions for  $c_1$  and  $c_2$  into Eq. (B.2) and simplifying leads to Eq. (25).

## References

- Antia, H.M., 2002. Numerical Methods for Scientists and Engineers, second ed. Birkhäuser-Verlag.
- Boulton, N.S., 1954. The drawdown of the water-table under non-steady conditions near a pumped well in an unconfined formation. In: Proceedings of the Institution of Civil Engineers, vol. 3, pp. 564–579.
- Bruggeman, G.A., 1999. Analytical solutions of geohydrological problems. Developments in Water Science, vol. 46. Elsevier.
- Butler, J.J.J., Tsou, M.S., 2003. Pumping-induced leakage in a bounded aquifer: an example of a scale-invariant phenomenon. Water Resources Research 39 (12), 1344.
- Cooley, R.L., 1971. A finite difference method for unsteady flow in variably saturated porous media: application to a single pumping well. Water Resources Research 7 (6), 1607–1625.
- de Hoog, F.R., Knight, J.H., Stokes, A.N., 1982. An improved method for numerical inversion of Laplace transforms. SIAM Journal of Scientific and Statistical Computing 3 (3), 357–366.
- Doherty, J., 2002. Manual for PEST, fifth ed. Watermark Numerical Computing, Australia.
- Ehlig, C., Halepaska, J.C., 1976. A numerical study of confined–unconfined aquifers including effects of delayed yield and leakage. Water Resources Research 12 (6), 1175–1183.
- Favati, P., Lotti, G., Romani, F., 1991. Algorithm 691 improving QUADPACK automatic integration routines. ACM Transactions on Mathematical Software 17 (2), 218–232.
- Hantush, M.S., 1960. Modification of the theory of leaky aquifers. Journal of Geophysics 65 (11), 3713–3726.
- Hantush, M.S., 1964. Hydraulics of Wells. Advances in Hydro-science, vol. 1. Academic, New York, pp. 282–432.
- Hantush, M.S., Jacob, C.E., 1955. Nonsteady radial flow in an infinite leaky aquifer. Eos Transactions, AGU 36 (1), 95–100.
- Lenoach, B., Ramakrishnan, T.S., Thambynayagam, R.K.M., 2004. Transient flow of a compressible fluid in a connected layered permeable medium. Transport in Porous Media 57, 153–169.
- Li, Y., 2006. Numerical evaluation of analytical solution for a 5-layer aquifer–aquitard system with application to the Oxnard Basin in California. M.Sc. Thesis, University of Arizona, Tucson.
- Malama, B., Kuhlman, K.L., Barrash, W., 2007. Semi-analytical solution for flow in leaky unconfined aquifer–aquitard systems. Journal of Hydrology 346 (1–2), 59–68.
- Moench, A.F., 1994. Specific yield as determined by type-curve analysis of aquifer-test data. Ground Water 32 (6), 949–957.
- Neuman, S.P., 1972. Theory of flow in unconfined aquifers considering delayed response of the water table. Water Resources Research 8 (4), 1031–1045.
- Neuman, S.P., 1974. Effect of partial penetration on flow in unconfined aquifers considering delayed gravity response. Water Resources Research 10 (2), 303–312.
- Neuman, S.P., Witherspoon, P.A., 1969a. Applicability of current theories to flow in leaky aquifers. Water Resources Research 5 (4), 817–829.
- Neuman, S.P., Witherspoon, P.A., 1969b. Theory of flow in a confined two aquifer system. Water Resources Research 5 (3), 803–816.
- Sepulveda, N., 2008. Three-dimensional flow in the storative semiconfining layers of a leaky aquifer. Ground Water 46 (1), 144–155.
- Tartakovsky, G.D., Neuman, S.P., 2007. Three-dimensional saturated–unsaturated flow with axial symmetry to a partially penetrating well in a compressible unconfined aquifer. Water Resources Research 43, 1–17.
- Wieder, T., 1999. Algorithm 794: numerical HANKEL transform by the FORTRAN program HANKEL. ACM Transactions on Mathematical Software 25 (2), 240–250.
- Zhan, H., Bian, A., 2006. A method of calculating pumping induced leakage. Journal of Hydrology 328 (3–4), 659–667.
- Zlotnik, V.A., Zhan, H., 2005. Aquitard effect on drawdown in water table aquifers. Water Resources Research 41, W06022.